Effects of sacubitril-valsartan on remodelling, fibrosis and mitochondria in a murine model of isoproterenol-induced left ventricular dysfunction

Giuseppe Vergaro [a,b,*,1], Annamaria Del Franco [a,b,1], Alessandro Carecci [a], Yu Fu Ferrari Chen [a], Alberto Aimo [a,b], Francesca Forini [c], Giuseppina Nicolini [c], Claudia Kusmic [c], Francesco Faita [c], Vincenzo Castiglione [a,b], Vincenzo De Tata [d], Angela Pucci [d], Veronica Musetti [a], Silvia Burchielli [e], Claudio Passino [a,b], Michele Emdin [a,b]

[a] Division of Cardiology and Cardiovascular Medicine, Fondazione Toscana Gabriele Monasterio, Pisa, Italy
[b] Health Science Interdisciplinary Center, Scuola Superiore Sant'Anna, Pisa, Italy
[c] CNR Institute of Clinical Physiology, Pisa, Italy
[d] Translational Research on New Technologies in Medicine and Surgery, University of Pisa, Pisa, Italy
[e] Fondazione Toscana Gabriele Monasterio, Pisa, Italy

ARTICLE INFO

ABSTRACT

Background: Sacubitril/valsartan has been demonstrated to promote left ventricular (LV) reverse remodelling and improve outcomes in patients with heart failure (HF) with reduced ejection fraction (EF). Its molecular and tissue effects have not been fully elucidated yet, due to the paucity of preclinical studies, mostly based on ischaemic models. We aimed to evaluate the effects of sacubitril/valsartan on LV remodelling, myocardial fibrosis and mitochondrial biology in a murine model of non-ischaemic LV dysfunction.
Methods: Adult transgenic male mice with cardiac-specific hyperaldosteronism (AS mice) received subcutaneous isoproterenol injections to induce LV systolic dysfunction. After 7 days, mice were randomized to a 2-week treatment with saline (ISO-AS $n = 15$), valsartan (ISO + V $n = 12$) or sacubitril/valsartan (ISO + S/V n = 12). Echocardiography was performed at baseline, at day 7, and after each of the 2 weeks of treatment. After sacrifice at day 21, histological and immunochemical assays were performed. A control group of AS mice was also obtained (Ctrl-AS $n = 8$).
Results: Treatment with sacubitril/valsartan, but not with valsartan, induced a significant improvement in LVEF ($p = 0.009$ vs ISO-AS) and fractional shortening ($p = 0.032$ vs ISO-AS) after 2-week treatment. In both ISO + V and ISO + S/V groups, a trend toward reduction of the cardiac collagen 1/3 expression ratio was detected. ISO + V and ISO + S/V groups showed a significant recovery of mitochondrial morphology and inner membrane function meant for oxidative phosphorylation.
Conclusion: In a murine model of non-ischaemic HF, sacubitril/valsartan proved to have beneficial effects on LV systolic function, and on cardiac energetics, by improving mitochondrial activity.

1. Introduction

Activation of renin-angiotensin-aldosterone system is one of the main pathways involved in cardiovascular remodelling because of its vasoconstrictor, profibrotic and proinflammatory effects [1]. Pharmacological antagonism of renin-angiotensin-aldosterone system improves morbidity and mortality of patients with heart failure (HF) [2]. Nonetheless, a persistent activation of pro-inflammatory and neurohormonal

Fig. 1. Echocardiographic parameters at baseline-D0, treatment start-D1, intermediate evaluation-D2, treatment end-D3. AS mice were shown as: (Ctrl-AS) control $n = 8$; (ISO-AS) isoproterenol alone $n = 15$; (ISO + V) isoproterenol + valsartan $n = 12$; (ISO + S/V) isoproterenol + valsartan/sacubitril $n = 12$. (EDLVD) end diastolic left ventricular diameter; (EF) ejection fraction; (FS) fractional shortening; (ESLVD) end systolic left ventricular diameter. *$p \leq 0.05$ vs ISO-AS.

axes, with elevation of plasma renin activity [3–5] and aldosterone [6,7] can be observed despite therapeutic optimization. In a murine model of cardiac-specific hyperaldosteronism and isoproterenol-induced left ventricular (LV) dysfunction, canrenoate, a specific mineralocorticoid receptor antagonist, reduced - but did not suppress - inflammation and myocardial fibrosis [8].

Sacubitril/valsartan, a combined neprilysin and angiotensin receptor inhibitor [9] reduces mortality and HF hospitalizations compared to enalapril, in symptomatic patients with HF with reduced ejection fraction (EF <40%) [10]. Neprilysin represents the main mechanism of enzymatic clearance of natriuretic peptides, but also acts on other substrates, such as endothelin-1, substance P, angiotensin I and β-amyloid protein [11,12].

Beneficial effects of sacubitril/valsartan on myocardial fibrosis have been reported after 4 week-treatment in a murine model of post-ischaemic LV dysfunction [13], and on myocardial hypertrophy and inflammatory damage in spontaneously hypertensive rats [14]. Indeed, the positive effects on myocardial remodelling prove to be more evident

in the subset of HF with a non-ischaemic aetiology [15]. Still, despite the overwhelming evidence on clinical efficacy of sacubitril/valsartan [16], its molecular effects have not been fully elucidated. Moreover, whether sacubitril/valsartan improves myocardial energetics has never been investigated.

We aimed to evaluate the effects of sacubitril/valsartan on LV remodelling, myocardial fibrosis and mitochondrial biology in a murine model of non-ischaemic LV dysfunction.

2. Methods

2.1. Animals

Adult transgenic male mice with cardiac-specific overexpression of the aldosterone synthase gene (α-MHC-AS mice on FVB background, hereinafter AS mice) and adult wild-type FVB male mice were used for the experimental protocol. As previously reported, AS mice overexpress the aldosterone synthase gene at the cardiac level and have a 2-fold increased cardiac aldosterone concentration [17]. Cardiac hyperaldosteronism results in an increased susceptibility to myocardial damage induced by isoproterenol infusion, thus leading to a decrease in LV fractional shortening and to a diffuse fibrosis [8].

2.2. Induction of LV systolic dysfunction and treatment

AS mice were treated with subcutaneous isoproterenol injections (300 mg/kg BID for 2 consecutive days D1-D2) to induce LV systolic dysfunction. The day before (D0) and five days after (D7) the last isoproterenol injection, a 2D-echocardiography was performed. At D8, mice were randomly assigned to a 2 week-treatment with saline (0.2 mL BID) (ISO-AS $n = 15$), valsartan (26 mg/kg by *oral gavage*) (ISO + V $n = 12$) or sacubitril/valsartan (57 mg/kg by *oral gavage*) (ISO + S/V n = 12). Echocardiography was repeated after the first week (D14) and at the end of treatment (D21). Mice were sacrificed at D21. As a control, a group of AS mice did not receive isoproterenol injection nor pharmacological treatment was obtained (Ctrl-AS $n = 8$) (Supplemental Fig. 1).
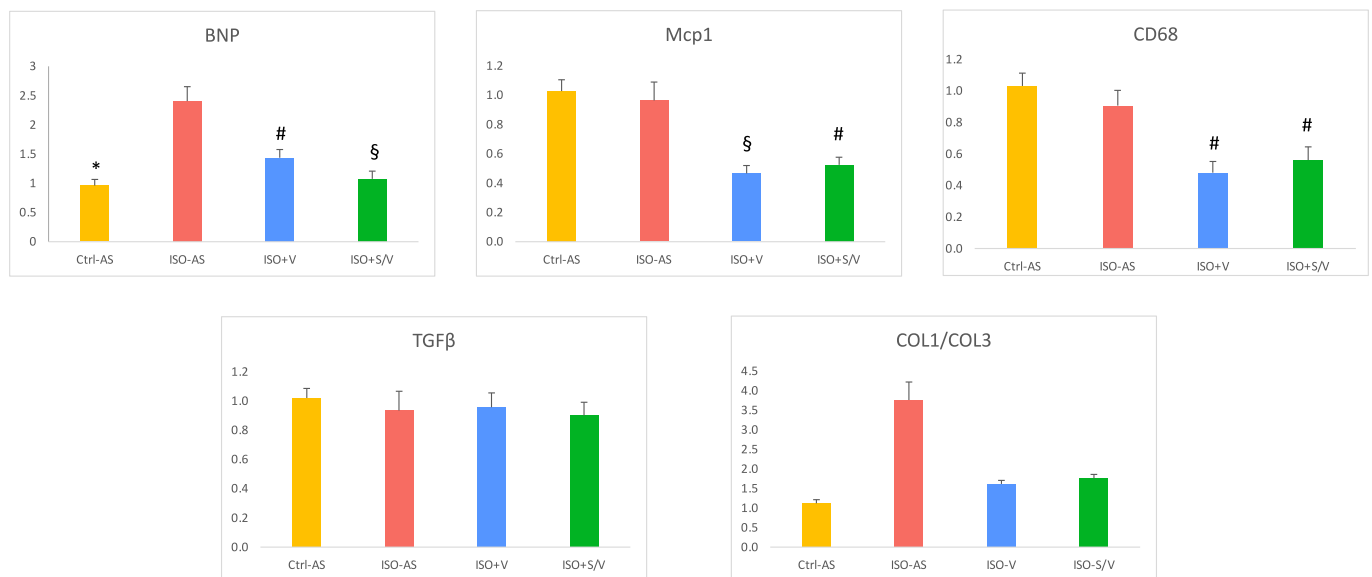
Fig. 2. Gene expression of markers cardiac stress, fibrosis and inflammation. Values were normalized to a control (Ctrl-AS) group composed of mice not induced with isoproterenol. Data are presented as mean ± SEM. * $p < 0.05$, # $p < 0.01$, § $p < 0.001$ vs ISO-AS, $n \geq 8$ animals per group.
(BNP) Brain natriuretic peptide; (CD68) Cluster of differentiation 68; (COL1–3) Collagen Type 1–3; (Mcp1) Monocyte chemoattractant protein 1; (TGF-β1) Transforming growth factor β1.
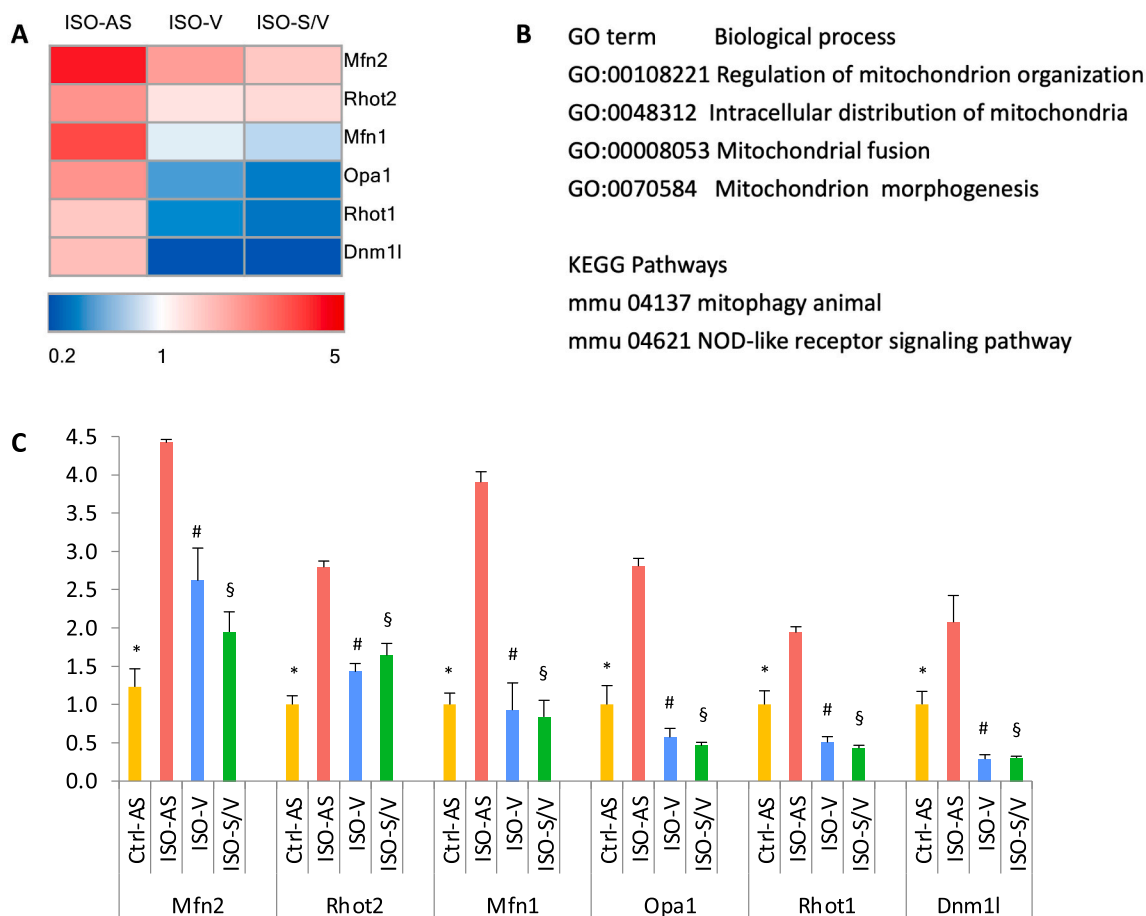
Fig. 3. Valsartan and sacubitril/valsartan counter-modulated genes involved in mitochondrial activity. A) Heat map examination of DE genes involved in the mitochondrial organization, distribution, and morphogenesis: values (fold change with respect to Ctrl-AS) were shown using colors and intensity of shading (blue = down-regulated, red = up-regulated). B) Significantly enriched biological processes and signalling pathways assessed by over-representation of gene ontology and KEGG pathways terms using the DE transcripts of the mitochondrial profiler array as input list. C) Histograms of DE genes involved in mitochondrial organization with $n \geq 3$ different animals per group. * $p \leq 0.03$, # $p \leq 0.002$, § $p < 0.0001$ vs ISO-AS.
(Dnm1l) Dynamin 1 Like; (Mfn1–2) Mitofusin 1–2; (Opa1) Optic atrophy type 1; (Rhot1–2) Ras Homolog Family Member T1–2. (For interpretation of the references to color in this figure legend, the reader is referred to the web version of this article.)

2.3. Echocardiography

Mice underwent bidimensional transthoracic echocardiography using a high-resolution ultrasound imaging system (Vevo 3100 - FUJI-FILM - VisualSonics Inc., Toronto, ON, Canada). Echocardiographic protocol required animal anesthetization with isoflurane (IsoFlo, Abbott Laboratories, Maidenhead, UK) by employing an induction chamber connected with a scavenger canister. After induction, each animal was located on a temperature-controlled board and left under anaesthesia during the examination (1–2% isoflurane in 1 L/min of pure oxygen), regulated to obtain heart rate (>400 bpm) comparable for every animal. Heart and respiratory rate, as well as body temperature, were constantly controlled by Advancing Physiological Monitoring Unit available with the imaging station (Vevo Imaging Station, FUJIFILM VisualSonics Inc., Toronto, Canada).

2D cardiac images were obtained in parasternal long and short axis view, while M-mode image was recorded at the papillary muscle level in short axis view. M-mode images were analysed with the software provided with the ultrasound equipment (VEVOLab, FUJIFILM Visual-Sonics Inc., Toronto, Canada), in order to measure LV fractional shortening, EF, LV mass, end-diastolic LV diameter, end-systolic LV diameter. All measurements were performed by two independent operators, in a blinded fashion.

2.4. Organ weight and tissue analysis

Mice were euthanized by means of an anaesthetic overdose (Sevo-flurane Piramal 100%). Body weight, heart weight, and tibia lengths were determined. The heart was transversally divided into two parts: the basal part was fixed in formalin, embedded in paraffin and then stained with Masson's trichrome; the apex was further divided into two parts: one was fixed for electron microscope observation, the other was snap frozen in liquid nitrogen and stored at -80 °C for molecular biology analysis. Evaluation of fibrosis was performed using a semiquantitative method. Total area of myocardial biopsy specimen was calculated for each sample. Interstitial fibrosis (on Masson's trichrome) areas were expressed as percentages of total sample area: 0 (absent), 1 (1%–5%), 2 (6%–15%), 3 (16%–30%) and 4 (>30%).

2.5. RNA extraction and cDNA synthesis

Total RNA was extracted from about 20 mg pulverized cardiac tissue using the miRNeasy Mini Kit (Qiagen) according to the manufacturer's instructions. To avoid DNA contamination, an on-column DNase digestion step was performed during the RNA extraction procedure by using the Invitrogen DNase reagent. A quantity of 1 μg RNA was reversed transcribed by using the QuantiTect Reverse Transcription Kit (Qiagen)
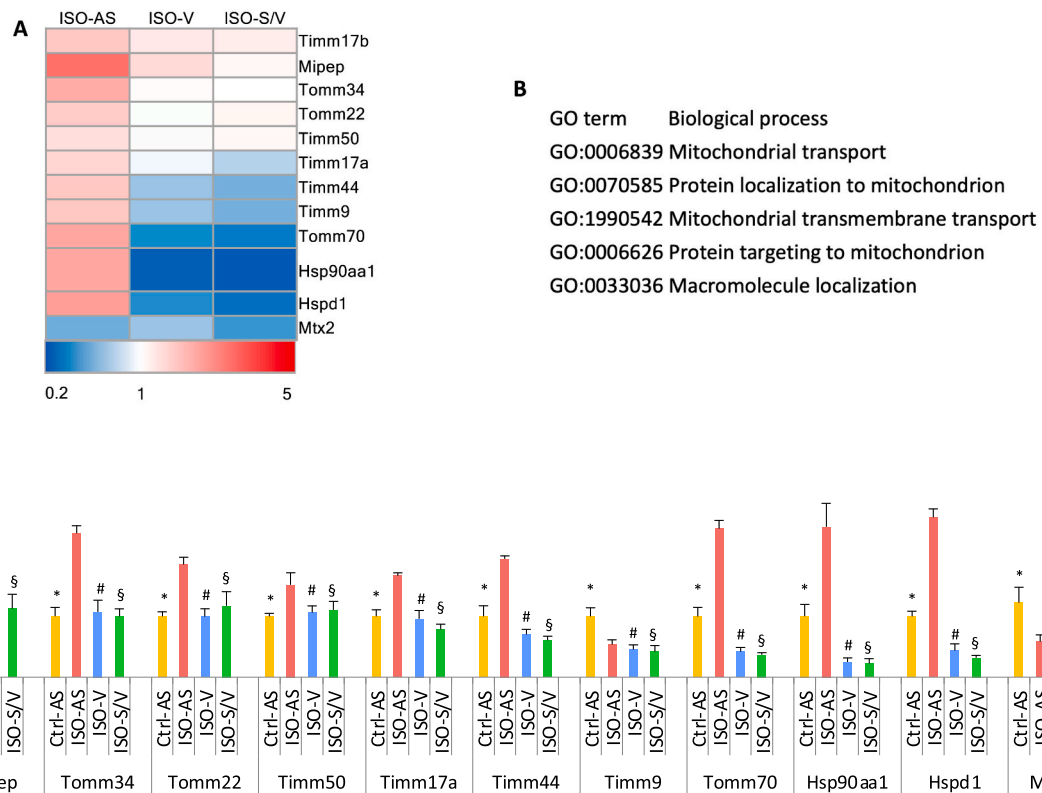
Fig. 4. Valsartan and sacubitril/valsartan counter modulated genes relevant to mitochondria protein transport. A) Heat map examination of DE genes involved in the mitochondrial protein transport, folding and maturation. Values (fold change with respect to Ctrl-AS) are shown using the same color legend of Fig. 6. B) Significantly enriched biological processes assessed by over-representation of gene ontology terms using the DE transcripts of the mitochondrial profiler array as input list. C) Histogram of DE genes involved in mitochondria protein import with n ≥ 3 different animals per group. * $p < 0.04$, # $p \leq 0.01$, § $p \leq 0.02$ vs ISO-AS. (Hsp90aa1) Heat Shock Protein 90 Alpha Family Class A Member 1; (Hspd1) Heat Shock Protein Family D Member 1; (Mipep) Mitochondrial Intermediate Peptidase; (Mtx2) Metaxin 2; (Timm9-17a-17b-44-50) Translocase Of Inner Mitochondrial Membrane 9-17a-17b-44-50; (Tomm22–34-70) Translocase Of Outer Mitochondrial Membrane22–34-70.

or the RT2 first strand Kit (Qiagen) for rt-PCR and PCR-array profiling respectively. Resulting cDNAs were stored frozen at −20 °C until assayed.

2.6. Quantitative reverse transcription - polymerase chain reaction

The quantitative reverse transcription - polymerase chain reaction was performed in triplicate in a total reaction volume of 20 μL in a Rotor-Gene Q real-time machine (Qiagen). The reaction mixture consisted of 3.5 μL H2O, 0.75 μL primers (10 μmol/L), 5 μL cDNA (2 ng/μL) and 10 μL Quantifast SYBR Green Mix (Qiagen). PCR was performed with 5 min of initial denaturation and then 40 cycles (for mRNA: 95 °C 10 s, 58 °C 20 s, 72 °C 10 s). After amplification, a melting curve analysis from 65 °C to 95 °C with a heating rate of 0.1 °C/s with a continuous fluorescence acquisition was constructed. The relative quantification of samples was performed by Rotor Gene Q-Series Software. Data were normalized against the mean of hydroxymethylbilane synthase and hypoxanthine guanine phosphoribosyltransferase housekeeping genes using the ΔΔ quantification cycle (ΔΔCq) method.

The primer sequences used were: brain natriuretic peptide (BNP) forward (5′- AGACCCAGGCAGAGTCAGAA −3′) and reverse (5′-CAGCTCTTGAAGGACCAAGG −3′); transforming growth factor β1 forward (5′- GTCAGCAGCCGGTTACCA −3′) and reverse (5′- GTCAG-CAGCCGGTTACCA −3′); collagen type 1 forward (5′-GCAGGTTCACCTACTCTGTCCT −3′) and reverse (5′- CTTGCCCCATT-CATTTGTCT −3′); collagen type 3 (Col3) forward (5′-TCCCCTGGAATCTGTGAATC -3′) and reverse (5′- TGAGTC-GAATTGGGGAGAAT −3′); monocyte chemoattractant protein 1

forward (5′- AGGTCCCTGTCATGCTTCTG −3′) and reverse (5′-TCTGGACCCATTCCTTCTTG −3′); cluster of differentiation 68 forward (5′- TTCTGCTGTGGAAATGCAAG −3′) and reverse (5′-AGAGGGGCTGGTAGGTTGAT −3′); hydroxymethylbilane synthase forward (5′- TCTAGATGGCTCAGATAGCATGCA-3′) and reverse (5′-TGGACCATCTTCTTGCTGAACA-3′); phosphoribosyltransferase forward (5′- AAGGACCTCTCGAAGTGTTGGATA −3′) and reverse (5′- CATT-TAAAAGGAACTGTTGACAACG -3′).

2.7. PCR array profiling

The PCR-array gene expression profiling was performed using the RT^2 Profiler™ PCR Array mouse plates dedicated to mitochondria gene panel (GeneGlobe ID - PARN-087Z), according to the manufacturer's instruction. Expression levels were quantified by SYBR Green chemistry in 96 well plates with a Biorad CFX96 Real-Time System. Each PCR-array plate contained quality control wells for assaying RNA quality, reverse transcription quality, PCR quality and DNA contamination. Cq analysis was performed by the BioRad CFX Manager software with a constant baseline adjustment of the relative fluorescent units for all array runs. Data were normalized against the mean of actine β, β2-microglobulin, glyceraldehyde 3-phosphate dehydrogenase, β-glucor-onidase and phosphoribosyltransferase housekeeping genes using the ΔΔCq method.

2.8. Gene ontology and pathways analysis

To elucidate mechanisms underlying mitochondrial homeostasis, we
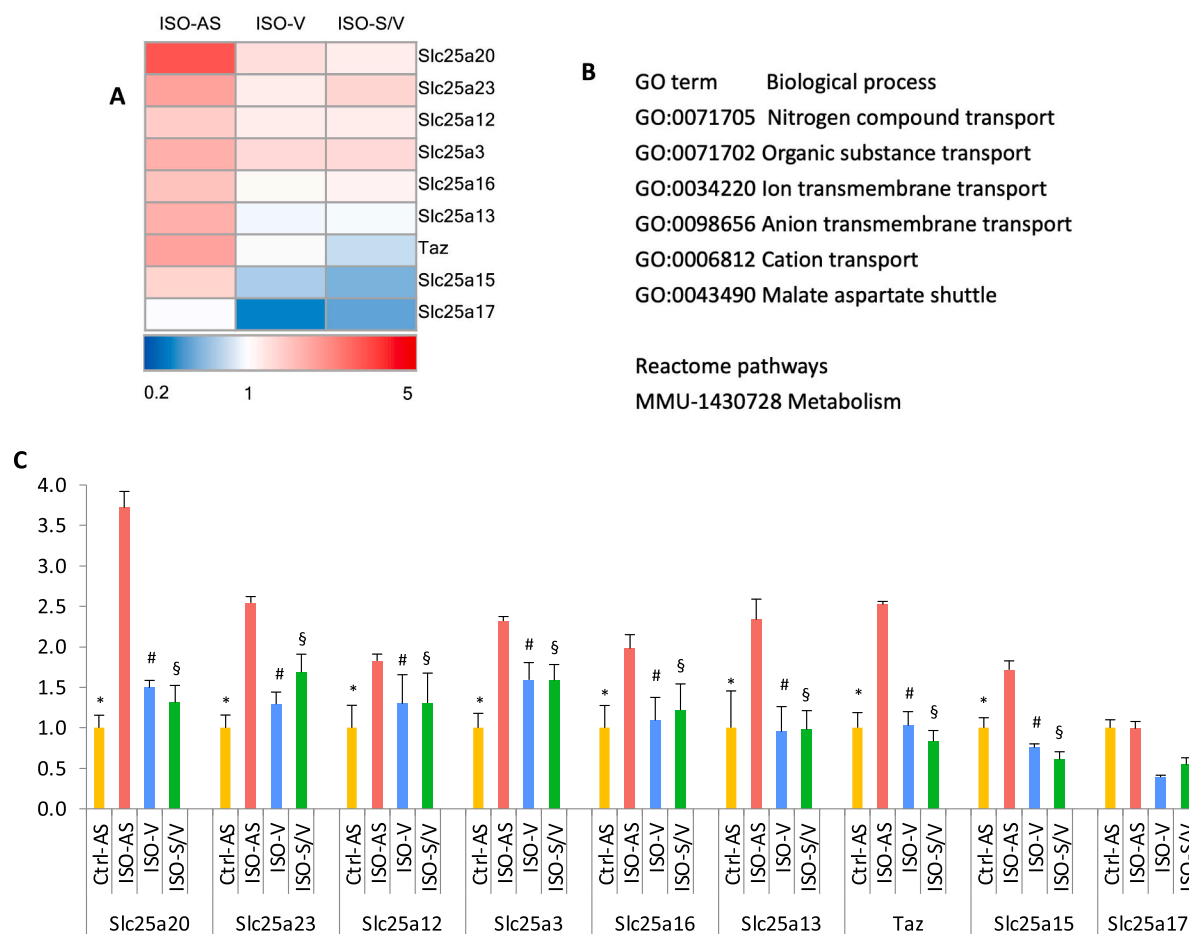
Fig. 5. Valsartan and sacubitril/valsartan counter modulated mitochondrial transport of organic/inorganic compounds. A) Heat map examination of DE genes involved in the mitochondrial transport of different solutes. Values (fold change with respect to Ctrl-AS) are shown using the same color legend of Fig. 6. B) Significantly enriched biological processes and signalling pathways assessed by over-representation of gene ontology and reactome pathways terms using the DE transcripts of the mitochondrial profiler array as input list. C) Histogram of DE genes involved in mitochondrial transport with n ≥ 3 different animals per group. * p < 0.05, # p < 0.05, § p < 0.05 vs ISO-AS.
(Slc25a3-a12-a13-a15-a16-a17-a20-a23) Solute Carrier Family 25 Member 3–12–13-15-16-17-20-23; (Taz) Tafazzin.

compared the expression of genes involved in the different cellular functions of mitochondria. To identify gene groups with similar biological function, we therefore performed an *in-silico* analysis of the main enriched biological processes and pathways using the differentially expressed (DE) genes implicated: 1) regulation of mitochondrial morphogenesis, dynamic and intracellular distribution (mitofusin 1–2, Ras homolog family member T1–2, optic atrophy type 1 and dynamin 1 like); 2) genes involved in the transport, maturation and insertion of mitochondrial proteins into the inner mitochondrial membrane (heat shock protein 90 alpha family class A member 1, heat shock protein family D member, mitochondrial intermediate peptidase, metaxin 2, translocase of inner mitochondrial membrane 9-17a-17b-44-50, translocase of outer mitochondrial membrane22–34-70); 3) mitochondrial transport of organic and inorganic compounds, as well as of metabolism (solute carrier family 25 member 3–12–13-15-16-17-20-23, tafazzin); 4) cardiac muscle cell death, apoptotic processes, autophagy and response to the superoxide (aryl hydrocarbon receptor interacting protein, B-cell lymphoma 2, B-cell lymphoma 2 L1, B-cell lymphoma 2 interacting protein 3, SH3 domain-containing GRB2-like protein B1, uncoupling protein 2–3).

Functional enrichment analysis of the biological processes (gene ontology terms), KEGG pathways and Reactome pathways was conducted in STRING database (https://string-db.org/) using as input the list of DE genes.
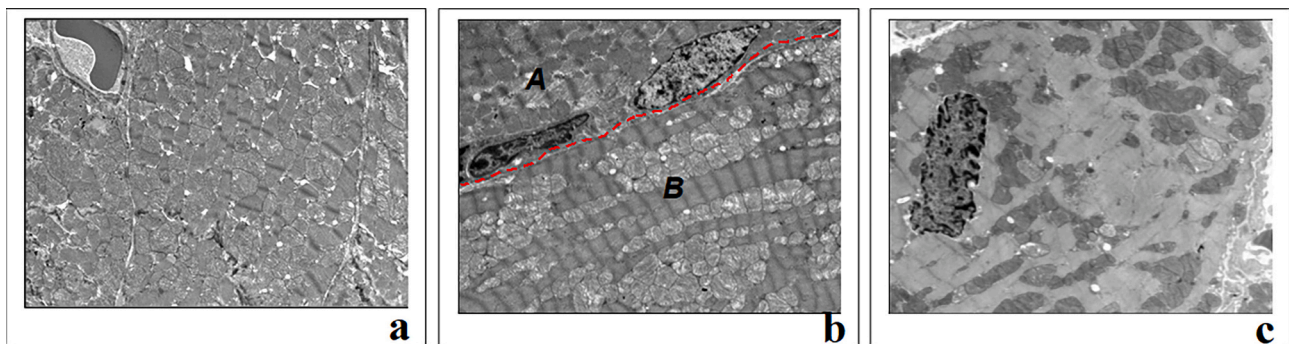
2.9. Electron microscopy

Freshly isolated cardiac samples extracted from LV were rinsed quickly in cold phosphate-buffered saline for the first hours, and then fixed with a glutaraldehyde–paraformaldehyde solution containing cacodylate buffer. After fixation, samples underwent a solvent-based dehydration step followed by embedding in epoxy resin, prior to ultra-fine sectioning and post-staining with heavy metal stains. The ultra-fine sectioning was performed using a ultramicrotome, obtaining sections of 1 μm that were cut and stained with toluidine blue. The samples were then cut further using a diamond knife in order to achieve sections of 50–70 nm, that were then placed onto a metal grid. Finally, a descriptive analysis was done with the examination of the cardiac ultra-structures and the description of the visual differences between samples.

2.10. Statistical analysis

Continuous variables were shown as mean ± standard error of the mean, whereas categorical variables as percentage. Data are also reported as mean and standard deviation in Supplemental Tables 1–5. Comparison between groups (Crtl-AS, ISO-AS, ISO + V, ISO + S/V) were performed using Kolmogorov-Smirnov test, χ square test and Kruskal-Wallis test, as appropriate. All gene expression data were normalized to control. Differences among groups were evaluated with one-way
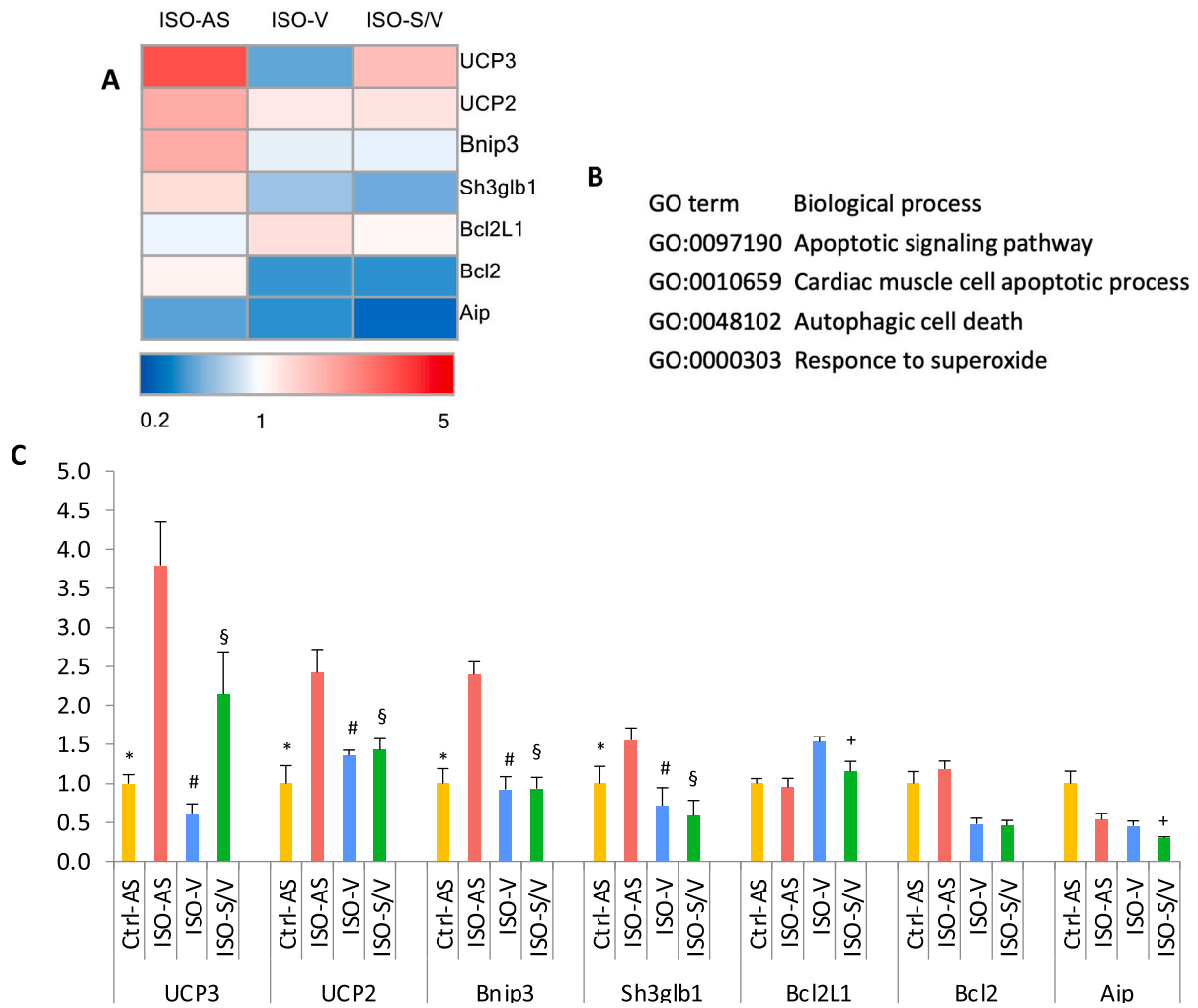
Fig. 6. Valsartan and sacubitril/valsartan regulated cell death/survival. A) Heat map examination of DE genes involved in the regulation of mitochondrial dependent cell death and autophagy. Values (fold change with respect to Ctrl-AS) are shown using the same color legend of Fig. 6. B) Significantly enriched biological processes assessed by over-representation of gene ontology terms using the DE transcripts of the mitochondrial profiler array as input list. C) Histogram of DE genes involved in cell death/autophagy with $n \geq 3$ different animals per group. * $p \leq 0.04$, # $p \leq 0.01$, § $p < 0.02$ vs ISO-AS. + $p < 0.05$ vs ISO + V.
(Aip) Aryl Hydrocarbon Receptor Interacting Protein; (Bcl2) B-cell lymphoma 2; (Bcl2L1) B-cell lymphoma 2 L1; (Bnip3) B-cell lymphoma 2 Interacting Protein 3; (Sh3glb1) SH3 domain-containing growth factor receptor-bound protein 2-like protein B1; (UCP2–3) Uncoupling protein 2–3.

Fig. 7. Ultrastructural characteristics of mitochondria at transmission electron microscopy. (a) ISO-AS cardiomyocytes with very dilated mitochondria, fragmented cristae, dilated sarcoplasmic reticulum and disorganization of myofibrillar complex. (b) ISO + V: Cardiomyocytes with predominantly regular ultrastructure. Specifically, [A] Sporadic cardiomyocytes [B] with alterations similar to ISO-AS: very dilated mitochondria presenting dispersed matrix and fragmented cristae, dilated sarcoplasmic reticulum. (c) ISO + S/V: cardiomyocytes with regular ultrastructure.

ANOVA, followed by Bonferroni post hoc correction. Differences were considered statistically significant at a value of $p < 0.05$.

3. Results

3.1. Sacubitril/valsartan improves isoproterenol-induced left ventricular systolic function and remodelling

ISO + S/V mice showed a higher LVEF ($p = 0.009$) and fractional shortening ($p = 0.032$) at the end of the observation period, compared to ISO-AS mice. These results matched with a reduction of end-systolic LV diameter at day 21 ($p = 0.032$) in mice with ISO + S/V (Fig. 1). Heart weight/tibia length ratio tended to be lower in the ISO + V and ISO + S/V compared the ISO-AS group, although this difference was not statistically significant (Supplemental Fig. 2). Data on heart rate during echocardiography are reported in Supplemental Table 6.

3.2. Effects of sacubitril/valsartan on myocardial fibrosis

Sacubitril/valsartan and valsartan treatments did not affect the extent of interstitial fibrosis at histological evaluation after 2 weeks of treatment ($p = 0.86$) (Supplemental Fig. 3). Collagen type 1/ collagen type 3 ratio was significantly higher in the ISO-AS mice compared to Crtl-AS ($p = 0.036$); only sacubitril/valsartan was associated with a trend in the reduction of collagen type 1/ collagen type 3 ratio ($p = 0.098$ ISO + S/V vs ISO-AS; $p = 0.24$ ISO + V vs ISO-AS). BNP gene expression was also lower in ISO + S/V and ISO + V groups compared to ISO-AS ($p < 0.01$). Further, biomarkers of inflammation (monocyte chemoattractant protein 1 and cluster of differentiation 68) were less expressed in ISO + S/V and in ISO + V than Ctrl-AS group ($p < 0.01$), as shown in Fig. 2.

3.3. Rescue of mitochondrial activity with sacubitril/valsartan

Compared to Ctrl-AS group, ISO-AS mice showed altered expression of 28 transcripts out of 53 total genes that gave an evaluable signal in the mitochondria profiler array (Figs. 3–6). Treatment with isoproterenol was associated with a dysregulation of the expression of genes linked to mitochondrial activity. This alteration was similarly rescued by valsartan or sacubitril/valsartan.

To predict the biological and functional implications of the observed gene expression changes, we performed a functional enrichment analysis of the 28 DE genes using the String annotation tool. DE genes were enriched into four main groups of biological processes of key relevance to mitochondrial quality control, metabolism and mitochondrial dependent death. The first group includes genes involved in the regulation of mitochondrial morphogenesis, dynamic and intracellular distribution such as: mitofusin 1–2, optic atrophy type 1, dynamin 1 like (essential for mitochondrial fusion and maintenance of mitochondrial morphology), and Ras homolog family member T1–2 (facilitating mitochondrial transport by attaching the mitochondria to the motor/adaptor complex) (Fig. 3).

Valsartan and sacubitril/valsartan also counter modulated genes involved in the transport, maturation and insertion of mitochondrial proteins into the inner mitochondrial membrane including: heat shock protein 90 alpha family class A member 1 and heat shock protein family D member (essential for the folding and assembly of newly imported proteins in the mitochondria), mitochondrial intermediate peptidase (involved in the maturation of oxidative phosphorylation - OXPHOS-related proteins), metaxin 2 (involved in the import of proteins into the mitochondrion), translocase of inner mitochondrial membrane 9-17a-17b-44-50 and translocase of outer mitochondrial membrane 22–34-70 (translocases located respectively in the inner, and outer mitochondrial membrane) (Fig. 4). A third group of DE genes with similar function is relevant to mitochondrial transport of organic and inorganic compounds, as well as to metabolism, including some

members of solute carrier family 25 (solute carrier family 25 member 3–12–13-15-16-17-20-23) and tafazzin, a novel stimulator for mitochondrial biogenesis (Fig. 5). Finally, valsartan and sacubitril/valsartan regulated genes relevant to cardiac muscle cell death and survival, apoptotic processes, autophagy and response to the superoxide such as: the anti-apoptotic aryl hydrocarbon receptor interacting protein and B-cell lymphoma 2, the proapoptotic B-cell lymphoma 2 interacting protein 3, SH3 domain-containing growth factor receptor-bound protein 2-like protein B1 (also involved in autophagosome formation), and uncoupling protein 2–3 (implicated in response to oxidative stress and in dissociating oxidative phosphorylation from ATP synthesis) (Fig. 6).

3.4. Restoration of ultrastructural characteristics of mitochondria with sacubitril/valsartan treatment

In ISO-AS group, cardiomyocytes showed markedly dilated mitochondria associated with dispersed matrix, fragmented cristae and dilated sarcoplasmic reticulum; the myofibrillar complex appeared disorganized, in part due to the encumbrance related to mitochondrial dilatation (Fig. 7a). Samples obtained from ISO + V mice showed a partial recovery of mitochondrial morphology, while samples from ISO + S/V mice exhibited a full recovery (Fig. 7b-c). Specifically, in the ISO + V and ISO + S/V groups, cardiomyocytes displayed regular ultrastructure, and their mitochondria showed physiological sizes and morphology, except few cases (almost 1% of mitochondria in a single cardiomyocyte) that were so dilated as to appear as giant mitochondria.

4. Discussion

In our study we analysed the effects of treatment with sacubitril/valsartan or valsartan in reverting cardiac remodelling and mitochondrial biology in a murine model of non-ischaemic HF. Sacubitril/valsartan was superior to valsartan in ameliorating LV systolic function after 2-week treatment, while sacubitril/valsartan and valsartan similarly remodulated the expression of genes relevant to mitochondrial function and morphology, which may anticipate the effects on LV structure and function and possibly contribute to their clinical effectiveness [18].

In patients with HF with reduced EF, sacubitril/valsartan has been shown to reduce both end-diastolic and end-systolic volume [16]. Reverse remodelling is indeed often a result of neurohormonal antagonism, and is correlated with a more favourable outcome [19]. In our model, treatment with sacubitril/valsartan was associated with an improvement in LV systolic function, that was mainly related to a decrease of end-systolic LV diameter. Modifications of systolic diameters, usually precede other changes in a context of reduced afterload [20], thus a reduction in diastolic diameters may be expected with longer treatment periods. The more pronounced effects of sacubitril/valsartan compared to valsartan on cardiac remodelling may be likely due to neprilysin inhibition [19].

The beneficial effects of sacubitril/valsartan also include the reduction of cardiac hypertrophy and fibrosis, in non-ischaemic HF [21]. Although a trend toward reduction was observed both for myocardial fibrosis at histology and for collagen gene expression after valsartan/sacubitril treatment, we could not find conclusive results for myocardial fibrosis. The initiation of pharmacological treatment 1-week after isoproterenol injections may explain these findings, as nor valsartan nor sacubitril-valsartan may revert established fibrosis.

According to the energy starvation hypothesis [22], the altered myocardial metabolism anticipates, triggers, and supports the contractile dysfunction of the heart [23], and has gained importance as one of the primary goals of HF therapies. Patients with HF show a reduction of mitochondrial function in cardiac tissue, as indicated by the low capacity in mitochondrial oxygen consumption [24]. Moreover, mitochondrial abnormalities in HF lead not only to a reduced capacity to generate adenosine triphosphate, but also to cardiomyocyte injury and

death [25]. Mitochondrial biology represents, therefore, an important potential therapeutic target in patients with HF. In particular, therapeutic strategies may be focused on "mitoprotection", restoring the homeostasis in mitochondrial fission and fusion, in particular in acute settings, such as post-acute myocardial infarction HF [26]. In our paper, we performed a dedicated analysis of the effects of sacubitril/valsartan on cardiac mitochondrial function. We report that sacubitril/valsartan and valsartan treatment proved to revert the adverse morphological alterations induced by isoproterenol and to ameliorate mitochondrial homeostasis at various levels. Mice treated with sacubitril/valsartan or valsartan showed a recovery of mitochondrial size, cristae, and matrix aspect. Further, they showed a rescue of expression of the genes involved in maintenance of mitochondrial morphology and function. With this regard, isoproterenol injection induces an altered expression of the genes involved in mitochondrial distribution, transport of organic and inorganic compounds, myocardial cell death, and response to superoxide. All these negative effects were partially reverted by both sacubitril/valsartan or valsartan treatment. Our results are in agreement with findings of a recent study [27], reporting that valsartan or sacubitril/valsartan treatment contribute to the normalization of mitochondrial homeostasis and gets along with the well-known decrease of oxidative stress associated with sacubitril/valsartan treatment in HF [28]. Exploration of other indices of mitochondrial function in future experimental studies to directly investigate the impact of sacubitril/valsartan treatment on mitochondrial function about cardioprotection: in particular, as sacubitril/valsartan has demonstrated to regulate the expression of genes involved in different mitochondrial activities, it could be interesting to analyze the effect of this drug on the function of oxidative phosphorylation by high-resolution fluorespirometry [28] or mitochondrial complex I-IV respiration with a Clark type electrode, ATP production with ATP assays mix, ROS formation measured with the amplex red hydrogen peroxide assays, calcium retention capacity and extramitochondrial calcium concentration [29], and the aggregation state of the respiratory complexes [30]. This analysis can be performed using different substrates, such as isolated mitochondria, tissue homogenates, intact cells [28] or permealized cells [31,32], The confirmation of the beneficial effects of sacubitril/valsartan on cardiac energetics in our murine models should be promoted in a human cohort.

There are limitations to be disclosed. First, the short observation period may not be sufficient to demonstrate the effects of sacubitril/valsartan on myocardial remodelling. However, we focused on early effects on pharmacological treatment, and on possible additional value of sacubitril/valsartan over valsartan. Further, the shortest treatment period reasonably associated to an effect on remodelling was chosen to minimize the suffering of animals. Second, we did not explore functional activity of mitochondria, since we analysed the activation of the various pathways in which mitochondria are involved without evaluating energy production in terms of adenosine triphosphate.

5. Conclusion

Sacubitril/valsartan treatment proves to early induce an amelioration of LV systolic function and to counteract detrimental changes in mitochondrial morphology and altered transcriptional signature relevant to mitochondrial biology in a murine model of non-ischaemic dilated cardiomyopathy. Our results provide evidence that the beneficial effects of sacubitril/valsartan may be participated by an improvement of mitochondrial biology.

Supplementary data to this article can be found online at https://doi.org/10.1016/j.ijcard.2024.132203.

Ethical considerations

Ethical approval was granted for this study by the Italian Ministry of Health for animal experiments (authorization number 92/2018-PR).

Author statement

CRediT authorship contribution statement

Giuseppe Vergaro: Writing – original draft, Project administration, Investigation, Formal analysis, Data curation, Conceptualization. **Annamaria Del Franco:** Writing – original draft, Project administration, Methodology, Investigation, Formal analysis, Data curation, Conceptualization. **Alessandro Carecci:** Investigation, Data curation. **Yu Fu Ferrari Chen:** Writing – original draft, Methodology, Investigation. **Alberto Aimo:** Writing – original draft, Methodology, Investigation, Formal analysis. **Giuseppina Nicolini:** Writing – review & editing, Methodology, Formal analysis. **Francesco Faita:** Supervision, Project administration, Conceptualization. **Vincenzo Castiglione:** Writing – review & editing, Methodology, Conceptualization. **Vincenzo De Tata:** Writing – review & editing, Investigation, Formal analysis, Data curation. **Angela Pucci:** Writing – review & editing, Methodology, Investigation. **Veronica Musetti:** Methodology, Investigation, Data curation. **Silvia Burchielli:** Supervision, Methodology, Investigation. **Claudio Passino:** Supervision, Formal analysis, Conceptualization. **Michele Emdin:** Writing – review & editing, Supervision, Project administration, Funding acquisition, Conceptualization.

Declaration of competing interest

The authors have nothing to declare.

Data availability

The data underlying this article will be shared on reasonable request to the corresponding author.

References

[1] V.J. Dzau, Tissue renin-angiotensin system in myocardial hypertrophy and failure, Arch. Intern. Med. 153 (1993) 937–942 (PMID: 8386920).

[2] F. Shearer, C.C. Lang, A.D. Struthers, Renin-angiotensin-aldosterone system inhibitors in heart failure, Clin. Pharmacol. Ther. 94 (2013) 459–467.

[3] S. Masson, S. Solomon, L. Angelici, R. Latini, I.S. Anand, M. Prescott, A. P. Maggioni, G. Tognoni, J.N. Cohn, Val-Heft investigators. Plasma renin activity predicts adverse outcome in chronic heart failure, independently of pharmacologic therapy: data from the valsartan heart failure trial (Val-HeFT), J. Card. Fail. 16 (2010) 964–970.

[4] G. Vergaro, M. Emdin, A. Iervasi, L. Zyw, A. Gabutti, R. Poletti, C. Mammini, A. Giannoni, M. Fontana, C. Passino, Prognostic value of plasma renin activity in heart failure, Am. J. Cardiol. 108 (2011) 246–251.

[5] R. Poletti, G. Vergaro, L. Zyw, C. Prontera, C. Passino, M. Emdin, Prognostic value of plasma renin activity in heart failure patients with chronic kidney disease, Int. J. Cardiol. 167 (2013) 711–715.

[6] A.D. Struthers, The clinical implications of aldosterone escape in congestive heart failure, Eur. J. Heart Fail. 6 (2004) 539–545.

[7] G. Vergaro, C. Fatini, E. Sticchi, C. Vassalle, G. Gensini, A. Ripoli, P. Rossignol, C. Passino, M. Emdin, R. Abbate, Refractory hyperaldosteronism in heart failure is associated with plasma renin activity and angiotensinogen polymorphism, J. Cardiovasc. Med. (Hagerstown) 16 (2015) 416–422.

[8] G. Vergaro, M. Prud'homme, L. Fazal, R. Merval, C. Passino, M. Emdin, J. L. Samuel, A. Cohen Solal, C. Delcayre, Inhibition of Galectin-3 pathway prevents isoproterenol-induced left ventricular dysfunction and fibrosis in mice, Hypertension 67 (2016) 606–612.

[9] O. Vardeny, R. Miller, S.D. Solomon, Combined neprilysin and renin-angiotensin system inhibition for the treatment of heart failure, JACC Heart Fail. 2 (2014) 663–670.

[10] J.J. McMurray, M. Packer, A.S. Desai, J. Gong, M.P. Lefkowitz, A.R. Rizkala, J. L. Rouleau, V.C. Shi, S.D. Solomon, K. Swedberg, et al., Angiotensin-neprilysin inhibition versus enalapril in heart failure, N. Engl. J. Med. 371 (2014) 993–1004.

[11] A.J. Kenny, A. Bourne, J. Ingram, Hydrolysis of human and pig brain natriuretic peptides, urodilatin, C-type natriuretic peptide and some C-receptor ligands by endopeptidase-24.11, Biochem. J. 291 (1993) 83–88.

[12] C. Oefner, A. D'Arcy, M. Hennig, F.K. Winkler, G.E. Dale, Structure of human neutral endopeptidase (Neprilysin) complexed with phosphoramidon, J. Mol. Biol. 296 (2000) 341–349.

[13] T.G. von Lueder, B.H. Wang, A.R. Kompa, L. Huang, R. Webb, P. Jordaan, D. Atar, H. Krum, Angiotensin receptor neprilysin inhibitor LCZ696 attenuates cardiac remodeling and dysfunction after myocardial infarction by reducing cardiac fibrosis and hypertrophy, Circ. Heart Fail. 8 (2015 Jan) 71–78.

[14] H. Kusaka, D. Sueta, N. Koibuchi, Y. Hasegawa, T. Nakagawa, B. Lin, H. Ogawa, S. Kim-Mitsuyama, LCZ696, angiotensin II receptor-Neprilysin inhibitor, ameliorates high-salt-induced hypertension and cardiovascular injury more than valsartan alone, Am. J. Hypertens. 28 (2015) 1409–1417.

[15] Y.H. Lee, W.R. Chiou, C.Y. Hsu, P.L. Lin, H.W. Liang, F.P. Chung, C.T. Liao, W. Y. Lin, H.Y. Chang, Different left ventricular remodelling patterns and clinical outcomes between non-ischaemic and ischaemic aetiologies in heart failure patients receiving sacubitril/valsartan treatment, Eur. Heart J. Cardiovasc. Pharmacother. 8 (2022) 118–129.

[16] J.L. Januzzi Jr., M.F. Prescott, J. Butler, G.M. Felker, A.S. Maisel, K. McCague, A. Camacho, I.L. Piña, R.A. Rocha, A.M. Shah, et al., Association of change in N-terminal pro-B-type natriuretic peptide following initiation of Sacubitril-valsartan treatment with cardiac structure and function in patients with heart failure with reduced ejection fraction, JAMA 322 (2019) 1085–1095.

[17] A. Ganzevoort, J.K. Bendall, S. Fuchs, B. Escoubet, F. Rochais, J. Hoerter, J. Nehme, M. L. Ambroisine, N. De Angelis, G. Morineau, et al., Cardiac specific increase in aldosterone production induces coronary dysfunction in aldosterone synthase-transgenic mice, Circulation 110 (2004) 1819–1825.

[18] K.F. Docherty, M. Vaduganathan, S.D. Solomon, J.J.V. McMurray, Sacubitril/valsartan: Neprilysin inhibition 5 years after PARADIGM-HF, JACC Heart Fail. 8 (2020) 800–810.

[19] R.M. Burke, J.K. Lighthouse, D.M. Mickelsen, E.M. Small, Sacubitril/valsartan decreases cardiac fibrosis in left ventricle pressure overload by restoring PKG signaling in cardiac fibroblasts, Circ. Heart Fail. 12 (2019) e005565.

[20] T. Ihara, K. Komamura, Y.T. Shen, T.A. Patrick, I. Mirsky, R.P. Shannon, S. F. Vatner, Left ventricular systolic dysfunction precedes diastolic dysfunction during myocardial ischemia in conscious dogs, Am. J. Phys. 267 (1994) H333–H343.

[21] D.G. Kramer, T.A. Trikalinos, D.M. Kent, G.V. Antonopoulos, M.A. Konstam, J. E. Udelson, Quantitative evaluation of drug or device effects on ventricular remodeling as predictors of therapeutic effects on mortality in patients with heart failure and reduced ejection fraction: a meta-analytic approach, J. Am. Coll. Cardiol. 56 (2010) 392–406.

[22] S. Neubauer, The failing heart–an engine out of fuel, N. Engl. J. Med. 356 (2007) 1140–1151.

[23] J.S. Ingwall, Energy metabolism in heart failure and remodelling, Cardiovasc. Res. 81 (2009) 412–419.

[24] D.A. Brown, J.B. Perry, M.E. Allen, H.N. Sabbah, B.L. Stauffer, S.R. Shaikh, J. G. Cleland, W.S. Colucci, J. Butler, A.A. Voors, et al., Expert consensus document: mitochondrial function as a therapeutic target in heart failure, Nat. Rev. Cardiol. 14 (2017) 238–250.

[25] D. Ramaccini, V. Montoya-Uribe, F.J. Aan, L. Modesti, Y. Potes, M.R. Wieckowski, I. Krga, M. Glibetić, P. Pinton, C. Giorgi, et al., Mitochondrial function and dysfunction in dilated cardiomyopathy, Front. Cell Dev. Biol. 8 (2021) 624216.

[26] S. Hernandez-Resendiz, A. Prakash, S.J. Loo, et al., Targeting mitochondrial shape: at the heart of cardioprotection, Basic Res. Cardiol. 118 (2023) 49.

[27] X. Li, J. Braza, U. Mende, G. Choudhary, P. Zhang, Cardioprotective effects of early intervention with sacubitril/valsartan on pressure overloaded rat hearts, Sci. Rep. 11 (2021) 16542.

[28] D. Croteau, F. Qin, J.M. Chambers, E. Kallick, I. Luptak, M. Panagia, D.R. Pimentel, D.A. Siwik, W.S. Colucci, Differential effects of Sacubitril/valsartan on diastolic function in mice with obesity-related metabolic heart disease, JACC Basic Transl. Sci. 5 (2020) 916–927.

[29] C. Doerrier, L.F. Garcia-Souza, G. Krumschnabel, Y. Wohlfarter, A.T. Mészáros, E. Gnaiger, High-resolution FluoRespirometry and OXPHOS protocols for human cells, permeabilized fibers from small biopsies of muscle, and isolated mitochondria, Methods Mol. Biol. 1782 (2018) 31–70, https://doi.org/10.1007/978-1-4939-7831-1_3 (PMID: 29850993).

[30] H.R. Lieder, F. Braczko, N. Gedik, M. Stroetges, G. Heusch, P. Kleinbongard, Cardioprotection by post-conditioning with exogenous triiodothyronine in isolated perfused rat hearts and isolated adult rat cardiomyocytes, Basic Res. Cardiol. 116 (1) (2021 Apr 19) 27, https://doi.org/10.1007/s00395-021-00868-6. PMID: 33876304; PMCID: PMC8055637.

[31] R. Scrima, O. Cela, M. Rosiello, A.Q. Nabi, C. Piccoli, G. Capitanio, F.A. Tucci, A. Leone, G. Quarato, N. Capitanio, Mitochondrial sAC-cAMP-PKA Axis modulates the $\Delta\Psi$m-dependent control coefficients of the respiratory chain complexes: evidence of respirasome plasticity, Int. J. Mol. Sci. 24 (20) (2023 Oct 13) 15144, https://doi.org/10.3390/ijms242015144. PMID: 37894823; PMCID: PMC10607245.

[32] C. Eickelmann, H.R. Lieder, S.E. Shehada, M. Thielmann, G. Heusch, P. Kleinbongard, Mitochondrial respiration analysis in permeabilized porcine left ventricular and human right atrial specimens with ischemia-reperfusion, Am. J. Physiol. Heart Circ. Physiol. 325 (1) (2023 Jul 1) H125–H135, https://doi.org/10.1152/ajpheart.00172.2023. Epub 2023 May 26. PMID: 37235522.